Mon. Not. R. Astron. Soc. **000**, 000–000 (0000) Printed 2 July 2010 (MN LATEX style file v2.2)

An Improved Model for the Dynamical Evolution of Dark Matter Subhaloes

JianLing Gan[1,2,3⋆], Xi Kang[4,2], Frank C. van den Bosch[5], JinLiang Hou[1]
[1] *Key Laboratory for Research in Galaxies and Cosmology, Shanghai Astronomical Observatory, Chinese Academy of Sciences, 80 Nandan RD, Shanghai, 200030, China*
[2] *Max Planck Institute for Astronomy, Königstuhl 17, 69117 Heidelberg, Germany*
[3] *Graduate School of the Chinese Academy of Sciences, No.19A, Yuquan Rd., 100049 Beijing, China*
[4] *The Purple Mountain Observatory, 2 West Beijing Road, Nanjing 210008, China*
[5] *Department of Physics and Astronomy, University of Utah, 115 South 1400 East, Salt Lake City, UT 84112-0830*

arXiv:1007.0023v1 [astro-ph.CO] 30 Jun 2010

ABSTRACT
Using an analytical model, we study the evolution of subhalo, including its mass, angular momentum and merging time-scale. This model considers the dominant processes governing subhalo evolution, such as dynamical friction, tidal stripping and tidal heating. We find that in order to best match the evolution of angular momentum measured from N-body simulation, mass stripping by tidal force should become inefficient after subhalo has experienced a few passages of pericenter. It is also found that the often used Coulomb logarithm $\ln M/m$ has to be revised to best fit the merging time-scales from simulation. Combining the analytical model with the Extended Press-Schechter (EPS) based merger trees, we study the subhalo mass function, and their spatial distribution in a Milky-Way (MW) type halo. By tuning the tidal stripping efficiency, we can gain a better match to the subhalo mass function from simulation. The predicted distribution of subhaloes is found to agree with the distribution of MW satellites, but is more concentrated than the simulation results. The radial distribution of subhaloes depends weakly on subhaloes mass at both present day and the time of accretion, but strongly on the accretion time. Using the improved model, we measure the second moment of the subhalo occupation distribution, and it agrees well with the results of Kravtsov et al. (2004a) and Zheng et al. (2005).

Key words: methods: N-body simulations — galaxies: haloes — galaxies: mass function — cosmology: dark matter

1 INTRODUCTION

In the popular cold dark matter model, structure (dark matter halo) formation is processed in a hierarchical manner that small haloes form first, and they subsequently merge to form bigger haloes. The relics of merging haloes are seen as the normal galaxies in clusters, or dwarf satellites in the Milky-Way. In the context of galaxy formation, halo mergers play an important role, as they can significantly affect the star formation rate and morphology of galaxies. It is now widely accepted that elliptical galaxies are formed by major mergers (e.g., Toomre & Toomre 1972), and disk galaxies may experience preferentially minor mergers, or earlier major mergers if any. Thus one important aspect about galaxy formation in the cold dark matter (CDM) scenario is to understand how and when the mergers (halo merger) happen, how the mass and density profile of accreted haloes evolve, and what are their final fates: merge with central galaxies or get disrupted before sinking into the halo center.

The only appropriate way to study the properties of accreted haloes (subhaloes) is the fully dynamic-traced simulation. Earlier simulations (e.g., Katz & White 1993) suffer significant resolution effects, and they produce the overmerging pictures (e.g., Klypin et al. 1999; Moore et al. 1999). Simulations with higher resolution (Springel et al. 2001; Diemand et al. 2004; Gao et al. 2004b; Kang et al. 2005), especially the recent ones from two groups (Via Lactea: Diemand, Kuhlen & Madau 2007a; Aquarius: Springel et al. 2008) are shown to be capable of resolving subhalo down to very low mass and these simulations converged on the statistical distributions of subhaloes. For example, the subhalo mass function (SHMF) is found to be well described by a single power law in both low and high-mass host haloes. Normalized by the host halo mass, the SHMF is universal with a slight dependence on formation time of the host halo (Gao et al. 2004b; Kang et al. 2005; van den Bosch et al.

⋆ Email:jlgan@shao.ac.cn

2005). Those high-resolution N-body simulations also agree on the radial distribution of subhaloes and it is found to be shallower than the dark matter particles, and can be well fitted by an Einasto profile (e.g., Diemand et al. 2004; Springel et al. 2008). Other properties of subhaloes are also discussed but with diverse conclusions, such as the velocity bias of subhaloes, both a positive velocity bias (e.g., Diemand et al. 2004) and negative bias (Springel et al. 2001) are reported. The density profile of subhalo is rapidly truncated, with a higher concentration, but disagreements are hold for its inner density slope (Hayashi et al. 2003; Kazantzidis et al. 2004a; Diemand, Kuhlen & Madau 2007b; Springel et al. 2008).

In addition to the above statistical distributions of subhaloes, many studies also focus on their dynamical evolution. It is widely agreed that subhaloes will sink towards the host halo center by dynamical friction and gradually lose their mass due to tidal stripping. There are disagreement on the inner structure of subhaloes, especially at their late stages of evolution. Hayashi et al. (2003) found that subhaloes will redistribute their inner mass by tidal heating, and become disrupted soon once the tidal radius are smaller than their characteristic radius. Kazantzidis et al. (2004a) argued that the inner part of subhalo is resistant to tidal shock and subhalo can orbit in the host halo for a longer time. They pointed out that the rapid disruption of subhaloes is unsurprised if the initial conditions in simulations are not constructed in equilibrium. Kazantzidis et al. (2004b) further showed that numerical effects can also lead to rapid loss of mass from subhalo. Diemand et al. (2007b) found that subhaloes in their simulation can survive for longer time even after they have passed the very central part of host halo where the tidal force is very strong. The fate of subhalo is even more complicated by the presence of baryon. A few simulations (Gnedin et al. 2004; Nagai & Kravtsov 2005; Macciò et al. 2006; Weinberg et al. 2008; Dolag et al. 2009) have shown that compared to pure dark matter simulations, smooth particles hydrodynamic (SPH) simulations with baryon will leave more subhaloes in the host center as the condensation of baryon cores makes subhaloes more resistant to tidal disruption, and produce a radial distribution of subhaloes similar to that observed for the Milky Way satellites.

Among the studies of subhalo dynamical evolution, one important issue is how long it takes for a subhalo to sink into the center of its host halo. This is very important for the model of galaxy formation as it determines when the mergers of galaxies actually happen. This time-scale is often called as the dynamical friction time scales ($T_{\rm df}$). $T_{\rm df}$ was firstly derived by Binney & Tremaine (1987, hereafter BT87) and Lacey & Cole (1993) based on the Chandrasekhar (1943) description. Early simulation (Navarro et al. 1995) found that the BT87 formula matches well with the simulation results. Recently Jiang et al. (2008) and Boylan-Kolchin et al. (2008, hereafter BK08) both find that the BT87 formula under-estimates the merger time-scales, and they point out that BT87 neglected the mass loss of subhalo during it evolution. But even the results of Jiang et al. (2008) and BK08 differ by a factor of two, and this diversity is from various effects. Jiang et al. (2008) use cosmological simulation with star formation and feedback, while BK08 use controlled two-halo merging simulation with pure dark matter. Also they adopt different definitions for galaxy/subhalo mergers.

Although numerical simulation is the only proper method to study the dynamical evolution of subhalo, useful insight into physical processes governing subhalo evolution can be gained from analytical model. Base on the pioneer work of Taylor & Babul (2001), the analytical model was well developed in the past years (Benson et al. 2002; van den Bosch et al. 2005; Taylor & Babul 2004; 2005a; 2005b; Zentner & Bullock 2003; Zentner et al. 2005). The model includes the main physical processes governing subhalo evolution: gravitational force, dynamical friction, tidal stripping, tidal heating and disruption. Coupled with merger trees from the extended Press-Schechter (EPS) theory, the analytical model is capable of producing realistic catalogue of subhaloes in given host halo, which can be directly compared to N-body simulation results. Up to now most of these analytical works unfortunately neglect the study of subhalo merging time-scales. Although Taffoni et al. (2003) derived an fitting formula for $T_{\rm df}$, their results are not tested against simulation results. BK08 recently found that their results are still quantitatively inconsistent with the prediction of Taffoni et al. (2003).

In this paper, using an analytical model similar to Zentner et al. (2005; hereafter Z05), we study the dynamical evolution of subhalo. We investigate the effects of tidal stripping, Coulomb logarithm on the angular momentum[1] evolution, merging time-scale of subhalo. By comparing our model predictions to the simulation results of BK08, we proposed a modified Coulomb logarithm which can well reproduce the evolution of angular momentum and merging time-scales for subhalo with different mass ratio and orbit eccentricity. We then combine the analytical model with the Monte Carlo merger tree to produce subhalo catalogue in a Milky Way (MW) type halo, and compare the model predictions to both N-body simulation results and observed distribution of satellites in the Milky Way. In Section 2 we present the main ingredients of the analytical model and show the model predictions in Section 3. In Section 4 we further examine our model with the halo occupation distribution of subhaloes. In section 5 we discuss the radial distribution of subhaloes, and we briefly conclude our model in Section 6.

Throughout this paper we adopt a flat ΛCDM cosmology with the following cosmological parameters: $\Omega_{\rm m} = 0.25$, $\Omega_\Lambda = 0.75$, $h = H_0/(100\,{\rm km\,s^{-1}\,Mpc^{-1}}) = 0.73$, $\Omega_{\rm b} = 0.04$, $n_{\rm s} = 0.951$ and $\sigma_8 = 0.9$.

2 THE MODEL

In this section we present the model for the evolution of the population of dark matter subhaloes. The first part describes the merger history (i.e. mass assembly) of the host halo, which can be obtained using either the EPS theory or N-body simulations. The second part describes the dynamical evolution of subhaloes, and includes orbit integration in the presence of dynamical friction combined with tidal stripping and heating. Our model is similar to that of Z05,

[1] Throughout this paper, when referring to the angular momentum, we mean it is the angular momentum per unit mass or the specific angular momentum.

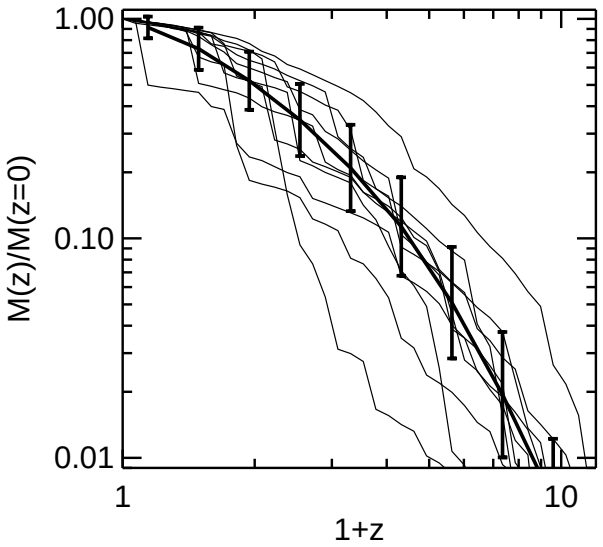

Figure 1. The 10 random mass accretion histories (MAHs, thin lines) for the mass of the main haloes as function of time, for a MW sized halo with $M(z=0) = 1.77 \times 10^{12} h^{-1} M_\odot$. The thick line with error bars show the average MAH and $1-\sigma$ scatters from 100 such realizations.

but there are also a few differences. We employ the well-calibrated code of Parkinson et al. (2008) to construct the EPS merger trees. This code is a significant improvement over the Somerville & Kolatt (1999) implementation used by Z05. In addition, we calibrate our model using detailed numerical simulations on the evolution of the orbital angular momentum of subhaloes. As we will demonstrate, this kind of calibration is far more constraining than using the mass function or velocity function of subhaloes. Finally, we (i) use a more detailed, empirical treatment of tidal heating, based on the results of high resolution numerical simulations, (ii) investigate the impact of changes in the Coulomb logarithm used in the analytical treatment of dynamical friction, and (iii) consider a different treatment for the tidal mass loss of subhaloes.

In what follows, we use m and M to denote the instantaneous masses of subhalo and host halo, respectively. Unless stated otherwise, we consider it understood that both m and M are functions of time. Then we use the symbol μ to refer to the mass ratio between subhalo and host halo, i.e., $\mu = \mu(t) = m(t)/M(t)$, without writing the time-dependence explicitly. We use $\mu_{\rm i}$, $\mu_{\rm f}$ to refer to the initial mass ratio at the time of accretion ($t_{\rm acc}$ or $z_{\rm acc}$) and the final mass ratio at present day ($z=0$), i.e., $\mu_{\rm i} = m(t_{\rm acc})/M(t_{\rm acc})$, $\mu_{\rm f} = m(z=0)/M(z=0)$, respectively.

2.1 Merger Trees

The backbone for modeling the population of dark matter subhaloes is the merger history of the host halo, which describes when each subhalo is accreted, and what its mass is at accretion. Halo merger histories can be obtained using N-body simulations, or in a semi-analytical fashion from the EPS formalism (Bond et al. 1991; Lacey & Cole 1993). Here we adopt the latter approach by employing the open-source code of Parkinson et al. (2008) to generate the assembly histories of MW sized haloes with a $z=0$ mass of $M(z=0) = 1.77 \times 10^{12} M_\odot$ that is close to the $z=0$ mass of the host halo in "Via Lactea" and "Aquarius" simulations. We construct 100 independent merger-tree realizations, each with a resolution of $10^8 M_\odot$. In Fig. 1 we show an example of the halo mass accretion history (MAH), which is defined as the mass of the most massive progenitors at each redshift from the merger tree. The thin lines are 10 random MAHs of the MW type halo in our adopted cosmology. The thick line with error bars is the average MAH and its $1-\sigma$ scatters (standard deviation) from 100 such realizations.

The main branch of the merger tree is defined as the trajectory of the most massive progenitors starting from the $z=0$ halo. In our study we consider only those haloes that are directly accreted onto the main branch, not accounting for any of their subhaloes (which would give rise to sub-subhaloes). As shown by Yang, Mo & van den Bosch (2009), sub-subhaloes (and higher-order substructures) only contribute a small fraction to the total substructure mass function (see also Giocoli et al. 2010).

For each halo in the merger trees, its virial radius, $r_{\rm vir}$, is defined as the radius within which the mean mass density is $\Delta_{\rm c}(z)$ times the critical density of the universe at redshift z, where

$$\Delta_{\rm c}(z) = 18\pi^2 + 82x - 39x^2 \qquad (1)$$

with $x = \Omega_{\rm m}(z) - 1$ (Bryan & Norman 1998). We assume that the host haloes are spheres with a density distribution given by the NFW profile (Navarro et al. 1997). The corresponding concentration parameter, c, is set using the median relation between c and halo mass M of Neto et al. (2007), which is given by

$$c(M,z) = \frac{4.67}{1+z}\left[\frac{M(z)}{10^{14}h^{-1}M_\odot}\right]^{-0.11}, \qquad (2)$$

where the dependence on redshift is taken from Bullock et al. (2001). Dark matter subhaloes are assumed to have a similar NFW profile at their time of accretion (i.e., at the time they become a subhalo), but as described below (see Section 2.2.5), this density profile is subsequently modified due to tidal heating.

2.2 Dynamical Evolution of Subhaloes

2.2.1 Orbital Parameters

The first step for the dynamical evolution of dark matter subhaloes is to assign their orbital parameters at the time of accretion, $t_{\rm acc}$. We follow Z05 and draw the initial orbital energy and angular momentum from distributions that have been obtained from N-body simulations. In particular, we assume that each subhalo starts its orbit at the virial radius, $r_{\rm vir}$, of the host halo at the time of accretion with an orbital energy equal to that of a circular orbit of radius $\eta r_{\rm vir}$, where η is drawn randomly from a uniform distribution between $[0.6, 1.0]$ (see Z05). The initial specific angular momentum is parameterized as $j_{\rm init} = \varepsilon j_{\rm c}$, where $j_{\rm c}$ is the specific angular momentum of the circular orbit mentioned above and ε is called the orbital circularity (note that $0 \le \varepsilon \le 1$). Several studies (e.g., Benson 2005; Tormen 1997; Z05; Khochfar & Burkert 2006; Jiang et al. 2008) have measured the distri-

bution of ε, all reporting similar results. Here we use the distribution obtained by Jiang et al. (2008):

$$f(\varepsilon) = 2.77\varepsilon^{1.19}\,(1.55-\varepsilon)^{2.99}\ . \tag{3}$$

2.2.2 Dynamical Friction

We treat subhalo as test particle in the orbital evolution. In addition to the (radial) force due to the gravitational potential of the spherical NFW host halo, subhalo experience an effective force due to 'dynamical friction' caused by the gravitational interaction between subhalo and the background 'field' particles that make up the host halo. Chandrasekhar (1943) showed that if the distribution of background particles is infinite and homogeneous, one can obtain an analytical expression for the dynamical friction force by considering the cumulative effect of many *uncorrelated* two-body interactions[2] between the subject mass (in our case the subhalo) and the individual field particles. This is known as the Chandrasekhar dynamical friction force, which is given by

$$\mathbf{F}_{\rm df} = -4\pi\left(\frac{Gm}{v_{\rm orb}}\right)^2 \ln\Lambda\,\rho(<v_{\rm orb})\frac{\mathbf{v}_{\rm orb}}{v_{\rm orb}}\,. \tag{4}$$

Here m and $v_{\rm orb}$ are the mass[3] and orbital velocity of the subhalo, $\ln\Lambda$ is the Coulomb logarithm, and $\rho(<v_{\rm orb})$ is the density of the particles in the host halo that have a speed less than the velocity of the subhalo. The Coulomb logarithm is introduced to avoid divergence that arises from the assumption of an infinite, homogeneous sea of field particles.

Similar to the frictional drag in fluid mechanics, dynamical friction exerts a force always opposite to the motion. However, contrary to hydrodynamic friction, which always increases in strength when the velocity increases, the drag due to dynamical friction has a more complicated dependence on velocity. While $F_{\rm df}\propto v_{\rm orb}$ in the low $v_{\rm orb}$-limit, similar to hydrodynamic friction, one has that $F_{\rm df}\propto v_{\rm orb}^{-2}$ in the high $v_{\rm orb}$-limit. In what follows we assume that the 'field' particles that make up the host halo follow a locally Maxwellian velocity distribution. In that case, Equation (4) reduces to

$$\mathbf{F}_{\rm df} = -4\pi\left(\frac{Gm}{v_{\rm orb}}\right)^2 \ln\Lambda\,\rho(r)\left[{\rm erf}(X)-\frac{2X}{\sqrt{\pi}}e^{-X^2}\right]\frac{\mathbf{v}_{\rm orb}}{v_{\rm orb}} \tag{5}$$

(BT87), where $X=v_{\rm orb}/[\sqrt{2}\sigma(r)]$ with $\sigma(r)$ the local, one-dimensional velocity dispersion of the host halo at radius r, which can be solved using the Jeans equation (BT87; Cole & Lacey 1996) under the assumption that the stress tensor is isotropic[4].

2.2.3 Coulomb Logarithm

As shown by White (1976), in the case of an extended subject mass, as is the case for our subhalo, one has that

$$\ln\Lambda = \frac{1}{m^2}\int_0^{b_{\rm max}} I^2(b)\,b^3\,{\rm d}b \tag{6}$$

where

$$I(b) = \int_b^\infty \frac{m(r)\,{\rm d}r}{r^2\,(r^2-b^2)^{1/2}} \tag{7}$$

with $m(r)$ the subhalo mass profile. Here $b_{\rm max}$ is the maximum impact parameter considered, which is introduced in order to avoid divergence. This divergence, however, arises because Equation (4) is based on the (unrealistic) assumption of a homogeneous and infinite medium. In our case of a subhalo orbiting in a host halo, a logical value for $b_{\rm max}$ may appear to be the size of the host system, which is indeed what is often adopted. However, it is important to realize that strictly speaking Equation (4) is not valid for this case, and that there is no 'correct' value for the Coulomb logarithm. Hence, different forms for $\ln\Lambda$ have been adopted in the literature. Some authors treat the Coulomb logarithm as a constant (Velazquez & White 1999; Taylor & Babul 2001; Jardel & Sellwood 2009). Others claims that this yields a dynamical friction time, $T_{\rm df}$, defined as the timescale on which the subject mass looses its orbital angular momentum, that is too short, and advocate instead that $\ln\Lambda$ has to be time-dependent (e.g., Colpi et al. 1999; Hashimoto et al. 2003). A widely used form for the Coulomb logarithm is $\ln(M/m)$ or $\ln(1+M/m)$, where M and m are the instantaneous (time-dependent) mass of the host and subhalo, respectively (e.g. BK08; Jiang et al. 2008). In this paper we will consider two different forms for the Coulomb logarithm: $\ln\Lambda = C$ and $\ln\Lambda = -\ln\mu + C$. As we will show, both forms yield equally satisfactory results (when compared to numerical simulations), as long as C is allowed to vary with the initial orbit parameters, η and ε, and the initial (i.e., at the time of infall) mass ratio $\mu_{\rm i}$.

2.2.4 Orbit Integration

We integrate the orbits $[\mathbf{x}(r,\theta)]$ of subhalo by treating it as test particle. The equation of motion for a subhalo of mass m is given by:

$$\frac{{\rm d}^2\mathbf{x}}{{\rm d}t^2} = -\frac{GM(<r)}{r^2}\,\frac{\mathbf{r}}{r} + \frac{\mathbf{F}_{\rm df}}{m} \tag{8}$$

with $M(<r)$ the mass of the host halo inside of radius r, and $\mathbf{F}_{\rm df}$ the dynamical friction force given by Equation (5). The equation of motion is solved using a fifth-order Cash-Karp Runga-Kutta method. During time-steps in which the mass of the host halo increases (due to the accretion of a new subhalo), we recompute the mass distribution and potential of the host halo, always under the assumption that the host halo has a NFW shape with the $c(M)$ relation as given by Equation (2). We assume that the orbital angular momentum of a subhalo is conserved when the mass of the host halo increases; the only mechanism by which the subhalo is assumed to lose orbital angular momentum is dynamical friction.

2.2.5 Tidal Stripping and Heating

When a subhalo orbits its host halo, it loses mass due to tidal stripping. The tidal radius, $r_{\rm t}$, is the radius in subhalo where the external differential (tidal) force from the

[2] By considering the interactions to be uncorrelated, one effectively ignores the self-gravity of the field particles.

[3] Note that the mass entering to the dynamical friction may not be the same as the bound mass of subhalo (e.g., Fellhauer & Lin 2007). Here, an 'effective' mass contributing to the dynamical friction is modeled.

[4] see Zentner & Bullock (2003) for a useful fitting function.

host halo exceeds the binding force of the subhalo, and is approximated by

$$r_{\rm t}^3 = \frac{Gm(<r_{\rm t})}{\omega^2 + G\left[2M(<r)/r^3 - 4\pi\rho(r)\right]}\,, \qquad (9)$$

with ω the angular speed of the subhalo and $\rho(r)$ the density profile of the host halo (von Hoerner 1957; King 1962; Taylor & Babul 2001). The subhalo mass outside $r_{\rm t}$ becomes unbound and is ultimately stripped. It should be pointed out, however, that Equation (9) is only a crude approximation. First of all, in the case of non-circular orbits the concept of a tidal radius is not well defined. Secondly, even in the case of point masses, the two-dimensional surface along which $\mathrm{d}^2 r_{\rm t}/\mathrm{d}t^2 = 0$ (i.e., zero-velocity surface; BT87) is not spherical, and so cannot be characterized by a single radius. And finally, Equation (9) ignores the orbital motion of particles within the subject mass. This, among other effects, gives rise to scatter in ω, and effectively introduces some non-zero 'thickness' to the shell of particles for which the internal and tidal forces balance.

Because of these uncertainties, numerical simulations show that many particles remain bound even though they lie beyond the tidal limit of Equation (9) when the subhalo is near pericenter (e.g., Diemand et al. 2007b). Fellhauer & Lin (2007) also showed that the previously stripped material can contribute to the dynamical friction and affect mass loss from the subhalo. This has resulted in uncertainties regarding how best to model tidal stripping. In particular, different studies adopt different time scales for tidal stripping, $T_{\rm strip}$, defined by

$$\frac{\mathrm{d}m}{\mathrm{d}t} = -\frac{m(>r_{\rm t})}{T_{\rm strip}}\,. \qquad (10)$$

Whereas Taylor & Babul (2001) simply assumed that $T_{\rm strip}$ is equal to the instantaneous orbital time $T_{\rm orb} \equiv 2\pi/\omega$, Z05 and Diemand et al. (2007b) inferred stripping time-scales that are 3.5 and 6 times shorter, respectively. In order to parameterize this uncertainty we adopt

$$T_{\rm strip} \equiv \frac{T_{\rm orb}}{A}\,, \qquad (11)$$

which we use in combination with Equations. (9) and (10) to describe mass loss due to tidal stripping. Here A is the tidal stripping efficiency parameter, which we tune using detailed numerical simulations (see Section 3.2 below). Note that Taylor & Babul (2001), Z05 and Diemand et al. (2007b) used or advocated $A \simeq 1.0$, 3.5 and 6.0, respectively.

Using numerical N-body simulations, it has been shown that tidal heating causes subhaloes to expand and to reduce their inner mass profile (e.g., Hayashi et al. 2003; Kravtsov et al. 2004b). Hayashi et al. (2003) introduced a modified NFW profile to describe the density distribution of a tidally heated subhalo according to

$$\rho(r) = \frac{f_{\rm t}}{1 + (r/r_{\rm te})^3}\rho_{\rm NFW}(r)\,. \qquad (12)$$

Here $\rho_{\rm NFW}(r)$ is the original NFW density profile of the subhalo at the time of infall, $r_{\rm te}$ is the 'effective' tidal radius that describes the outer cutoff imposed by the tides, and $f_{\rm t}$ describes the reduction in the central density of the subhalo. As shown by Hayashi et al. (2003), these are well-fit by

$$\lg\frac{r_{\rm te}}{r_{\rm s}} = 1.02 + 1.38\,Q_{\rm m} + 0.37\,Q_{\rm m}^2\,, \qquad (13)$$

and

$$\lg f_{\rm t} = -0.007 + 0.35\,Q_{\rm m} + 0.39\,Q_{\rm m}^2 + 0.23\,Q_{\rm m}^3\,. \qquad (14)$$

Here $Q_{\rm m} = \lg[m(t)/m(t_{\rm acc})]$ is the logarithm of the remaining fraction of subhalo mass, and $r_{\rm s}$ is the scale radius of the NFW profile at the time of accretion. Both $f_{\rm t}$ and $r_{\rm te}$ decrease with time while a subhalo is losing mass.

We caution that this 'empirical' treatment of tidal heating is subject to some debate. In particular, Kazantzidis et al. (2004a) have argued that the simulation used by Hayashi et al. (2003) was not set-up in equilibrium, and that this has resulted in a tidal mass loss rate that is too high. Unfortunately, lacking a more reliable description of how tidal heating impacts the density profiles of subhaloes, we use Equation (12) despite these potential problems.

2.2.6 Disruption and Cannibalism

As a subhalo is being exposed to tidal stripping and heating, it may reach a point at which it is disrupted, i.e., at which no significant amount of matter remains gravitationally bound into a single object. Alternately, depending on the dynamical friction time, a subhalo may either sink all the way to the center of the host halo's potential well (i.e., lose all its orbital angular momentum) or continue to orbit as a subhalo, if the mass ratio $m(t)/M(t)$ is such that dynamical friction is negligible.

Whether and when subhaloes are tidally disrupted is still being debated. Testing this with numerical simulations is complicated by the fact that simulations are always subject to numerical artifacts due to limited mass and force resolution. Using N-body simulations, Hayashi et al. (2003) found that subhaloes are disrupted once their tidal radius $r_{\rm t}$ becomes smaller than $\sim 2r_{\rm s}$. Motivated by these findings, Taylor & Babul (2004) and Z05 included tidal disruption in their semi-analytical models. They considered a subhalo to become tidally disrupted once its mass becomes less than its initial mass (i.e. at accretion) within a radius $f_{\rm dis}r_{\rm s}$, with $f_{\rm dis} = 0.1$ (Taylor & Babul 2004) and $f_{\rm dis} = 1.0$ (Z05), respectively. Using the luminosity function of Milky Way satellites, Macciò et al. (2009) argued that $0.1 \lesssim f_{\rm dis} \lesssim 0.5$, while Wetzel & White (2010), using a wide variety of observational constraints on satellite galaxies, conclude that subhaloes are disrupted once their bound mass drops below ~ 2 percent of its mass at infall, corresponding to $f_{\rm dis} \sim 0.3$ for a NFW profile with a concentration $c = 10$. Hence, typical values for $f_{\rm dis}$ that have been adopted in the literature cover the entire range $0.1 \lesssim f_{\rm dis} \lesssim 2$; as nicely shown by Wetzel & White (2010), varying $f_{\rm dis}$ by this amount has a huge impact on the radial number density distribution of surviving subhaloes, with smaller $f_{\rm dis}$ resulting in a more concentrated profile.

There have also been a number of studies that have argued that subhalo disruption is actually extremely rare. In particular, a number of numerical simulations with very high spatial resolution have shown that subhaloes are remarkably resilient to disruption by tidal shocks (e.g., Kazantzidis et al. 2004a; Bullock & Johnston 2005; Peñarrubia et al. 2008; Springel et al. 2008). Kanzantzidis et al. (2004a) argued that the initial conditions of the simulation of Hayashi et al. (2003) were not in equilibrium, which is likely to have caused a subhalo disruption rate that is too high. Using the

"Via Lactea" simulation, Diemand et al. (2007b) found that only very few subhaloes get disrupted; In their simulation 97% of the subhaloes identified at $z = 1$ were still present at $z = 0$, and even subhaloes with $r_{\rm t} < 0.2r_{\rm s}$ were found to survive. Finally, BK08 also found that subhaloes survive as bound entities up to the point of having lost all their orbital angular momentum (private communication).

Motivated by these high-resolution simulations, we assume that subhaloes are never disrupted. Rather, when a subhalo has lost all its orbital angular momentum, we consider it 'cannibalized' by (or 'merged' with) the host halo, and we remove the subhalo from our sample[5]. The merging time scale, $T_{\rm df}$, is defined as the time interval between accretion and merging of a subhalo. We consider two cases for subhalo mass loss due to tidal stripping. In the first case (hereafter Model M1), subhaloes can lose mass continuously until they are cannibalized by their host halo. In the second case (hereafter Model M2), tidal stripping is 'turned off' after a subhalo has experienced two pericentric passages. This is motivated by numerical simulations, which suggest that subhaloes only experience significant mass loss during their first two orbital periods (e.g., Diemand et al. 2007b). As we will show below (see Section 3.1), these two different treatments of tidal stripping yield very different predictions regarding the evolution of the orbital angular momentum of subhaloes.

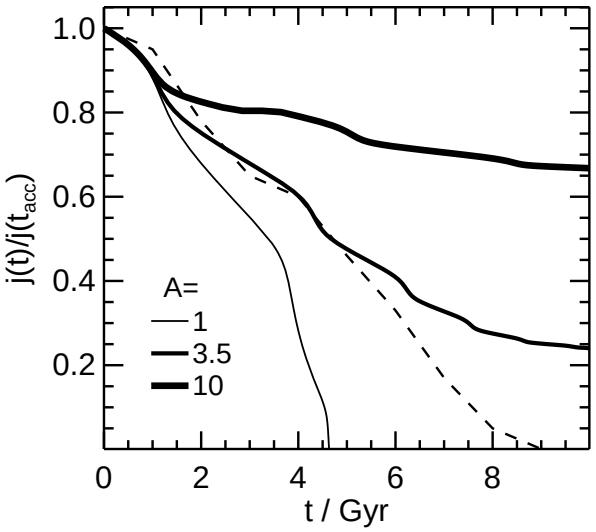

Figure 3. The evolution of angular momentum with $\mu_{\rm i} = 0.1$, $\varepsilon = 0.65$, $\eta = 1.0$, $\ln\Lambda = -\ln\mu$ from model M1. The solid lines are the model results with different tidal stripping efficiency ($A = 1, 3.5, 10$). The dashed line shows the simulation result from BK08.

3 COMPARISON WITH NUMERICAL SIMULATIONS

We now turn to a detailed comparison of our analytical model with numerical simulations. After exploring how the orbital evolution of a subhalo depends on the tidal stripping efficiency, A, and the Coulomb logarithm, $\ln\Lambda$, we tune these parameters by fitting the merging time-scales and the evolution of orbital angular momentum of subhaloes to the controlled, high-resolution numerical simulations of BK08. These simulations follow the orbital evolution of individual subhaloes of different mass and with different orbital properties in a host halo of fixed mass $M(t) = M$, and are ideally suited to tune our model parameters.

Subsequently, we use our model to compute the mass function and radial number density distribution of subhaloes in a MW type host halo, which we compare to numerical simulations and observational constraints from satellite galaxies in the MW.

3.1 Tuning the Tidal Stripping Efficiency and Coulomb Logarithm

Fig. 2 shows the evolution of the mass (upper panels) and halo-centric radius (lower panels; in units of the virial radius of the host halo) of a subhalo with $\mu_{\rm i} = 0.05$, $\varepsilon = 0.5$ and $\eta = 1.0$ in the model M1. In the left-hand panels the Coulomb logarithm is $\ln\Lambda = -\ln\mu$ and we vary the efficiency of tidal stripping, expressed by the parameter A (see Equation [11]), as indicated. Clearly, for larger values of A (i.e., more rapid mass loss), the effect of dynamical friction is reduced, and the orbital decay slows down drastically. With decreasing dynamical friction, subhalo can also travels to higher halo-centric radius (lower panel).

In the right-hand panels, we keep A fixed as 3.5 and vary the Coulomb logarithm, as indicated. Typically, a lower value for $\ln\Lambda$ results in dynamical friction being less efficient (cf. Equation [5]). This in turn implies a reduced mass loss, because the subhalo experiences fewer pericentric passages and, on average, more orbits at larger halo-centric radii where the tidal forces due to the host halo are weaker.

We now turn to a detailed comparison with the simulation results of BK08. To that extent, we use the same initial conditions, such as the density profiles of subhalo and host halo, orbital circularity and orbital energy. The dashed line in Fig. 3 shows the evolution of $j(t)$ for a subhalo with $\mu_{\rm i} = 0.1$, $\varepsilon = 0.65$, and $\eta = 1.0$ in the simulation of BK08. The solid lines show the predictions from our model M1, for three different values of A, as indicated. In all three cases we have used $\ln\Lambda = -\ln\mu$. Clearly, the evolution of orbital angular momentum is a strong function of the efficiency of tidal stripping, A. Larger values of A result in lower rate of angular momentum loss (i.e., a longer merging time scale, $T_{\rm df}$), simply because a less massive subhalo experiences weaker dynamical friction. Whereas our model with $A = 3.5$ matches $j(t)$ in the BK08 simulation reasonably well for the first ~ 5 Gyr, the predicted evolution in orbital angular momentum at later stages is too weak. We have experimented with different values of A but where unable to obtain a satisfactory match to the $j(t)$ in the simulation of BK08.

In Fig. 4, we investigate the impact of changing the Coulomb logarithm. In the left-hand panels we keep $\ln\Lambda$ fixed at some constant values (as indicated), while in the

[5] Note that some authors consider subhaloes 'merged' or 'cannibalized' when its separation from the host center is smaller than some fiducial radius (e.g., Kravtsov et al. 2004a; Z05). However, we consider our definition, based on the complete loss of orbital angular momentum, more realistic (see also BK08).

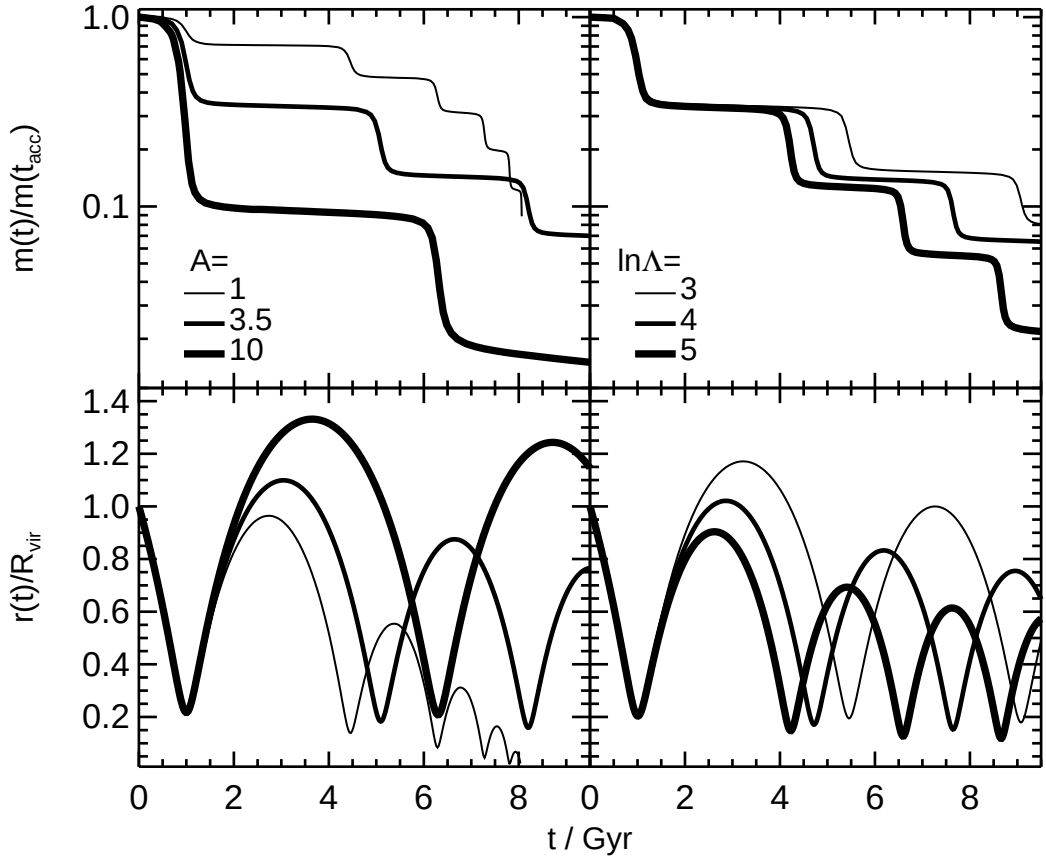

Figure 2. The evolution of mass and halo-centric radius for a subhalo with $\mu_{\rm i} = 0.05$, $\varepsilon = 0.5$, and $\eta = 1.0$ in model M1. In the left-hand panels, $\ln\Lambda = -\ln\mu$ and we vary the efficiency A of tidal stripping, as indicated. In the right-hand panels, $A = 3.5$ and we vary the value of the Coulomb logarithm, as indicated.

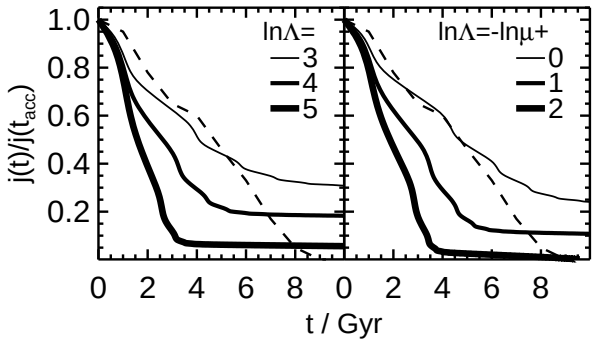

Figure 4. As Fig. 3, but with A is fixed as 3.5 (constrained from subhalo mass function, shown in Fig. 8). The figure shows the effects of varying Coulomb logarithm. Note the predicted slow evolution at later stages.

right-hand panels we adopt $\ln\Lambda = -\ln\mu + C$ for three different values of C (as indicated). In all case A is fixed as 3.5, which, as we will see in Section 3.2, yields a subhalo mass function that is in best agreement with numerical simulations. Although different Coulomb logarithms have a significant impact on the evolution of the orbital angular momentum, we were unable to find a form for $\ln\Lambda$ for which we could satisfactorily match the simulation results of BK08, even if we kept A a free parameter as well. The problem is that the model typically predicts a decline in the angular momentum loss rate, $\mathcal{R} \equiv -{\rm d}j/{\rm d}t$, while the simulation results have $\mathcal{R} \sim$ constant during the entire evolution, up to the point of being cannibalized by the host (i.e., when $j = 0$). The only exception is when the tidal stripping efficiency A is very low, in which case the merging time scale, $T_{\rm df}$, is much too short. The culprit for this discrepancy is the continued mass loss due to tidal stripping. This has motivated us to consider a modified model (model M2) in which tidal stripping is inefficient after two pericentric passages. As already mentioned above, this is not an entirely ad-hoc modification, as it has support from the ultra-high resolution "Via Lactea" simulation (Diemand et al. 2007b).

Fig. 5 shows the evolution of the orbital angular momentum of two different subhaloes from the model M2; in the upper panels $\mu_{\rm i} = 0.1$, $\varepsilon = 0.65$, and $\eta = 1.0$, while the lower panels correspond to a subhalo with the same η but with $\mu_{\rm i} = 0.05$ and $\varepsilon = 0.46$. The dashed lines indicate the results from the simulations of BK08, while the solid lines correspond to our model M2 with $A = 3.5$, and with the Coulomb logarithm tuned to best match the BK08 results. In the left- and right-hand panels we considered $\ln\Lambda = C$ and $\ln\Lambda = -\ln\mu + C$, respectively, where C is a constant. In all four cases, the fit to the $j(t)$ of BK08 is fairly satisfactory. Clearly, model M2 gives much better fit to the simulation results, and we adopt this model throughout the remainder of this paper (unless specifically stated otherwise).

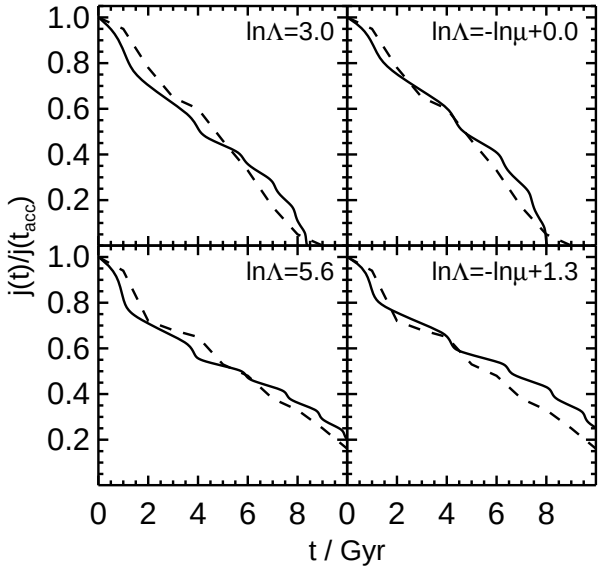

Figure 5. The evolution of angular momentum in model M2, in which tidal stripping is stopped after subhalo has gone through two pericenter passages. The upper panels are evolutions with $\mu_{\rm i} = 0.1$, $\varepsilon = 0.65$ and $\eta = 1.0$. Lower panels are for subhalo with $\mu_{\rm i} = 0.05$, $\varepsilon = 0.46$, $\eta = 1.0$. The two forms of Coulomb logarithm that $\ln\Lambda = C$ and $\ln\Lambda = -\ln\mu + C$ are used in left and right panels, respectively. The solid and dashed lines indicate the model and simulation (BK08) predictions. Better agreement between them can be obtained with appropriate $\ln\Lambda$.

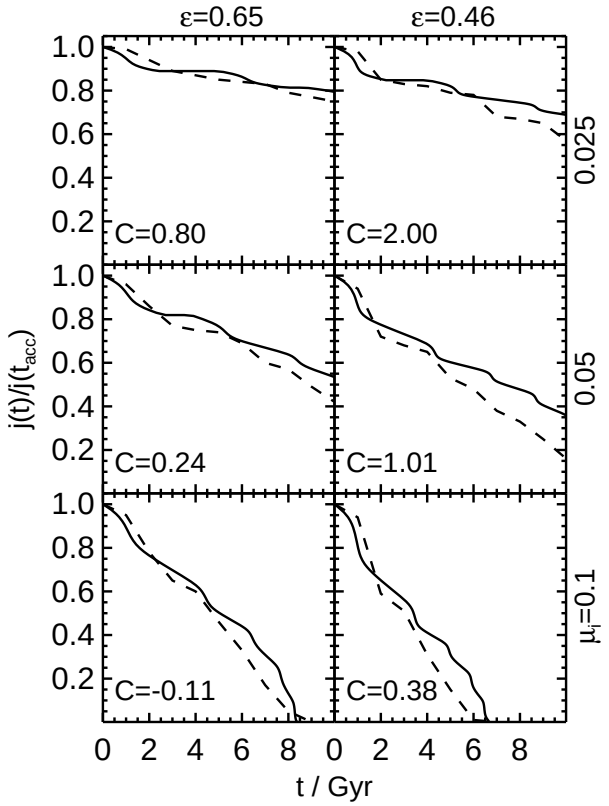

Figure 7. The evolution of angular momentum for subhalo. The dashed lines are from simulation by BK08, and solid lines are model predictions. Here the Coulomb logarithm is from Equation (15), and C is labeled in each panel. It shows that our revised Coulomb logarithm can well describe the evolution of angular momentum for subhaloes with different mass ratio, orbit circularity. $\eta = 1.0$ in all cases.

Note, though, that the best-fit value of C (indicated in each panel) is different in each case. Both the model with $\ln\Lambda = C$ and that with $\ln\Lambda = -\ln\mu + C$ yield equally satisfactory results. In what follows we will only consider the latter, since we believe it to be the more physical one. What remains to be done, however, is to characterize how C depends on the mass and orbital properties of the subhalo. Using a suite of numerical simulations, BK08 derived a fitting formula for the merging time scale, $T_{\rm df}$, as a function of the mass, m, the orbital circularity ε, and the orbital energy, η, of the subhalo at accretion. We use this fitting formula to constrain $C = C[\mu_{\rm i}, \eta, \varepsilon]$. After some experimenting, we finally adopted the following form for the Coulomb logarithm:

$$\ln\Lambda = -\ln\mu + c_1\mu_{\rm i}^{c_2}\eta^{c_3}\exp[c_4\varepsilon] + c_5\,. \qquad (15)$$

Fitting the merging time scales in our semi-analytical model to those listed in Table 1 of BK08, we obtain: $c_1 = 1.04$, $c_2 = -0.64$, $c_3 = 0.72$, $c_4 = -3.02$, and $c_5 = -0.75$.

Fig. 6 shows the merging time-scales as function of the initial mass ratio, $\mu_{\rm i}$, for three different values of the orbital circularity, as indicated in each panel. In all cases the initial orbital energy has $\eta = 1.0$, and we have adopted $A = 3.5$. The solid lines correspond to the predictions of model M2 using the above Coulomb logarithm of Equation (15), while the dashed lines indicate the fitting formula of BK08. Although not perfect, our model is in fair agreement with the simulation results of BK08. This is also evident from Fig. 7, where we show the evolution of orbital angular momentum for six different combinations of $\mu_{\rm i}$ and ε (as indicated). In each panel the dashed curve corresponds to the simulation results of BK08, while the solid line is our M2 model prediction based on the Coulomb logarithm of Equation (15). The corresponding value of C is indicated in each panel. Overall, our model yields $j(t)$ that are in satisfactory agreement with the simulation results of BK08.

3.2 The Distribution of Subhalo Population

In Section 2.2, we have introduced in detail the model for the evolution of subhalo, including its mass, radial position and merging time-scales. In Section 3.1, we tune the model parameters to fit the dynamical evolution of subhalo predicted by simulations. Couple with the merger trees, the model is ready to produce the subhalo catalogue in the host halo. As described in Section 2.1, our model employs 100 realizations of merger trees of the MW type halo, and each realization specifies a random assembly history of dark matter haloes (Fig. 1). We follow the dynamical evolution of the accreted subhaloes [with masses $m(z_{\rm acc}) \geq 10^8 M_\odot$] by the main branch of merger tree, and investigate the distribution of subhalo population at $z = 0$, including the subhalo mass function (SHMF) and their radial distribution. We also compare the model prediction with the simulation results and the observed distribution of the MW satellites.

Fig.8 show the SHMF and the radial number distribution in the upper and lower panels, respectively. For panels in each column, the same set of model parameters is used

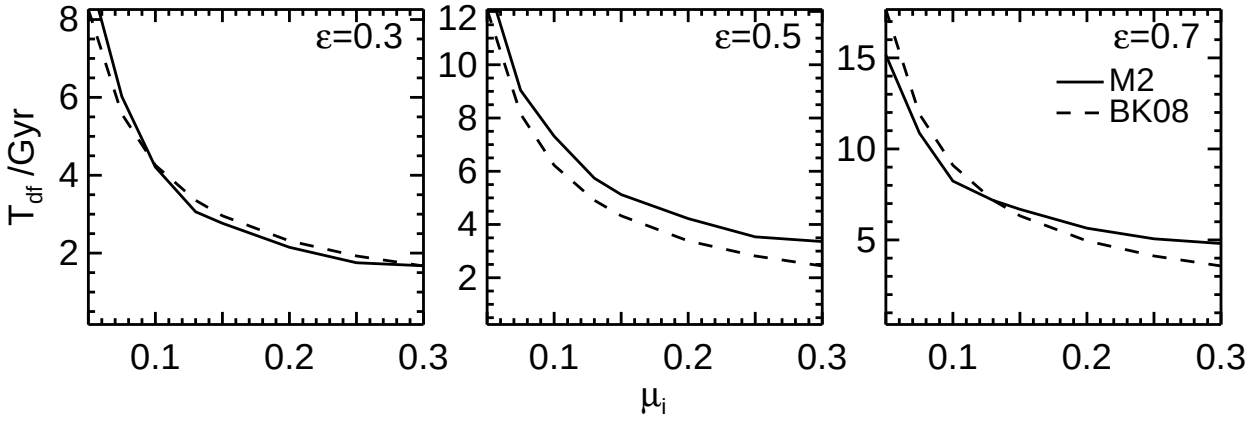

Figure 6. Subhalo merging time-scales. As in BK08, subhalo merges with central halo once it loses all of its angular momentum j. The three panels are for different orbital circularity $\varepsilon = 0.3, 0.5, 0.7$. The solid lines are from model M2 with $\eta = 1.0$, $A = 3.5$ and $\ln\Lambda = -\ln\mu + C$ given by Equation (15). The dashed line shows the fitting formula from simulations of BK08.

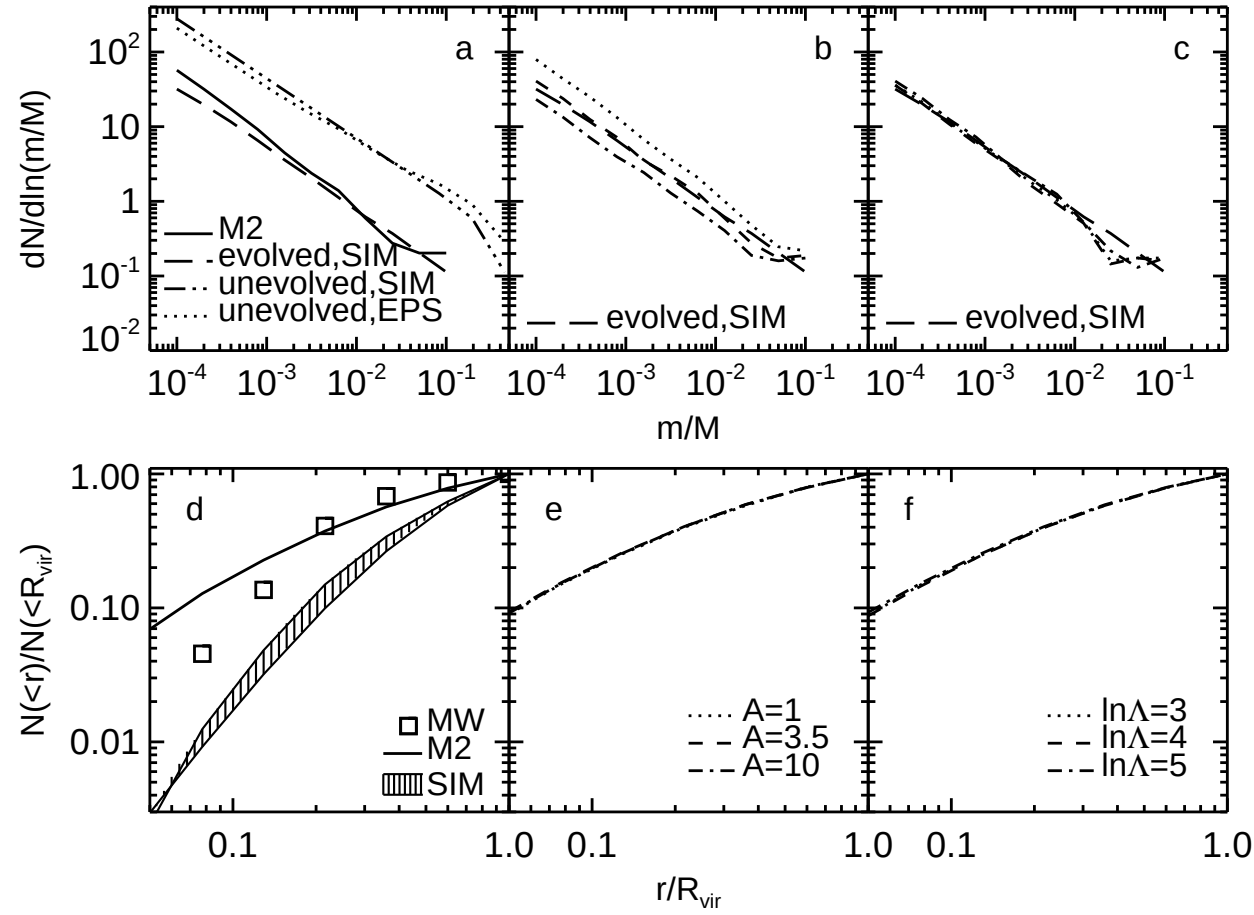

Figure 8. Subhalo mass function (SHMF, upper panels) and radial number distribution (lower panels) in a Milky-Way type halo. Panels a and d basically show the predictions from model M2 (solid) with $A = 3.5$ and Coulomb logarithm of Equation (15). In panel a, the unevolved and evolved SHMFs from simulation are shown as dashed-dotted and long dashed lines, respectively. In panel d, we also plot the radial number distribution of simulated subhaloes (hatch area, upper limit: Via Lactea; lower limit: Aquarius) and observational MW satellites (squares). In panels b and e, we compare the results of simulation to the model M1 with $\ln\Lambda = -\ln\mu$ and $A = 1, 3.5, 10$, while in panels c and f, the used parameters are $\ln\Lambda = 3, 4, 5$ and $A = 3.5$. The model predictions with different parameters are plotted in lines with varying line style as indicated.

and indicated in the lower panel. The SHMF from N-body simulations is well described by a power law, with index between -0.8 and -1.0 (Springel et al. 2001; Gao et al. 2004b; Kang et al. 2005; Diemand et al. 2004; Giocoli et al. 2008; 2010). In panel a, we show the simulated one from Giocoli et al. (2008) as the long-dashed line and the model prediction is shown as the solid line. It can be seen that our fiducial model (Model M2 with $A = 3.5$ and Coulomb logarithm from Equation (15)) produces a fair match to the simulation result.

As the SHMF is for an evolved population of accreted subhaloes, it is important to check if the unevolved SHMF, which is the mass function of subhaloes at their accretion times, is reproduced by the EPS based merger tree employed in our model. The unevolved SHMFs from simulation and the EPS model are shown as dashed-dotted and dotted lines, respectively. Their good agreement indicates that the model for the dynamical evolution of subhalo is not biased by the formation history of the host halo.

We further check if our model predictions are affected by the assumptions for the dynamical processes of subhalo. Panel b and c show the predictions from our Model M1, with the dependence on A (panel b) and Coulomb logarithm (panel c). It is found that the SHMF depends strongly on tidal stripping efficiency A, but weakly on Coulomb logarithm. This can be understood from that, as shown by van den Bosch et al. (2005), the subhaloes population at present day is dominated by the recent (the last $\sim 1-2$ Gyr) accretion history of the host halo. It is already shown in Fig. 2 that subhalo mass depends strongly on A at the first few Gyrs, but with a weak dependence on Coulomb logarithm. Thus the results indicate that SHMF can not be used to constrain the mass evolution of subhalo after a few Gyrs, while the dynamical evolution j can set strong constraints on the late stage evolution of subhalo, as shown in Section 3.1.

The radial number distribution of subhaloes is shown in the lower panels of Fig.8. In panel d, the hatched area shows the spanned distribution from simulations (upper limit: Via Lactea; lower limit: Aquarius). The observed distribution of the MW satellites is shown as the empty squares (data are from Mateo 1998; Kroupa et al. 2005; Metz et al. 2007; Metz et al. 2009; Martin et al. 2008). A clear discrepancy is that the distribution of the MW satellites is more concentrated than the subhaloes from N-body simulations, which has already been noted before (e.g. Taylor et al. 2005b). Such a discrepancy could be due to the incompleteness of observations (Willman et al. 2004), or the observed satellites present a biased population of subhaloes from simulations (Kravtsov et al. 2004b; Madau et al. 2008). We leave more discussion to Section 5.

The fiducial model prediction is shown as the solid line in panel d. Compared to the simulation result, the model predicts a more centrally concentrated distribution of subhaloes. A Similar discrepancy was also noted by Taylor & Babul (2005b) although their model prediction is slightly lower than ours. However, Z05 found that their model predicts a well match to simulation result, and they argued that the discrepancy noted by Taylor & Babul (2005b) is not from numerical effects of simulation but the model assumptions for subhalo merging and disruption. There still lacks detailed studies on this issue. Here we firstly explore if the predicted distribution of subhaloes is affected by the model assumption. The predictions from our Model M1 are shown in panel e and panel f, with dependence on A and Coulomb logarithm, respectively. Surprisingly, we find that the predicted distribution is similar to that obtained from our Model M2, and it also has no dependence on the model parameter A and $\ln\Lambda$.

In principle, the final spatial distribution of subhaloes is mainly determined by (1) their initial positions at accretion, (2) dynamical processes governing subhalo evolution, and (3) criteria on where and when subhalo disappears. The results in panel e and f suggest that (2) has no significant effects on the radial distribution of subhaloes. Since the low-mass subhaloes dominate the subhaloes population, varying the strength of the dynamical friction and tidal stripping will not change the spatial distribution of subhaloes much. In addition, Kang (2008) has shown that the formation history of the host halo from the EPS theory is very similar to that of simulations. As the mass and radius of halo are close related by Equation (1), the initial positions of subhaloes at accretion (the virial radius of host halo) from the EPS merger tree should be similar to the simulation results. Thus effect (1) will also contribute little to the discrepancy on the final radial distribution of subhaloes.

It is then reasonable to conclude that the over-predicted subhaloes at small radii is because either simulations still lack enough resolutions to resolve subhaloes in the central region of the host halo, or the model neglecting subhalo disruption is not realistic. With respect to simulation, Springel et al. (2008) have shown that increasing the resolution does resolve more low-mass subhaloes, but the number of subhaloes converges for given mass limit. Thus it is implausible that simulation resolution is responsible for this discrepancy. With respect to the model, defining a subhalo to be disrupted (or unbound) is very subjective, for example, most authors assume that subhalo is tidally disrupted if its mass is less than the initial mass within a radius $f_{dis}r_s$, but with a wide range of f_{dis} between $0.1 \sim 2.0$. As shown by Wetzel & White (2010), varying f_{dis} has a huge impacts on the final radial distribution of subhaloes.

In fact, there are more effects which can affect the abundance of subhaloes and their radial distribution. (i) Host halo formed in cosmological simulation always contains more than one subhalo, and the interaction between subhaloes will accelerate the disruption of subhaloes and reduce the number of subhaloes at the inner host halo (e.g., Tormen et al. 1998; Gnedin et al. 2004; Angulo et al. 2009). (ii) Ludlow et al. (2009) have shown that small subhaloes are more likely to be ejected out to larger distances during the virialization of the host halo, thus producing a less concentrated distribution. (iii) Subhalo-subhalo mergers may be also effective to reduce the abundance of subhaloes (e.g., Kim et al. 2009), especially for the less massive subhaloes (e.g., Angulo et al. 2009). Unfortunately, these processes are difficult to be included in the analytical model.

Finally in this section we consider the dependence of subhalo radial distribution on their properties. Most N-body simulations have shown that the radial distribution of subhaloes has no dependence on the present-mass of subhaloes (e.g., Gao et al. 2004b; Diemand et al. 2004; Springel et al. 2008), while others (e.g., De Lucia et al. 2004) found non-negligible dependence on subhalo mass. In Fig. 9 we show the fiducial model predictions with dependence on the

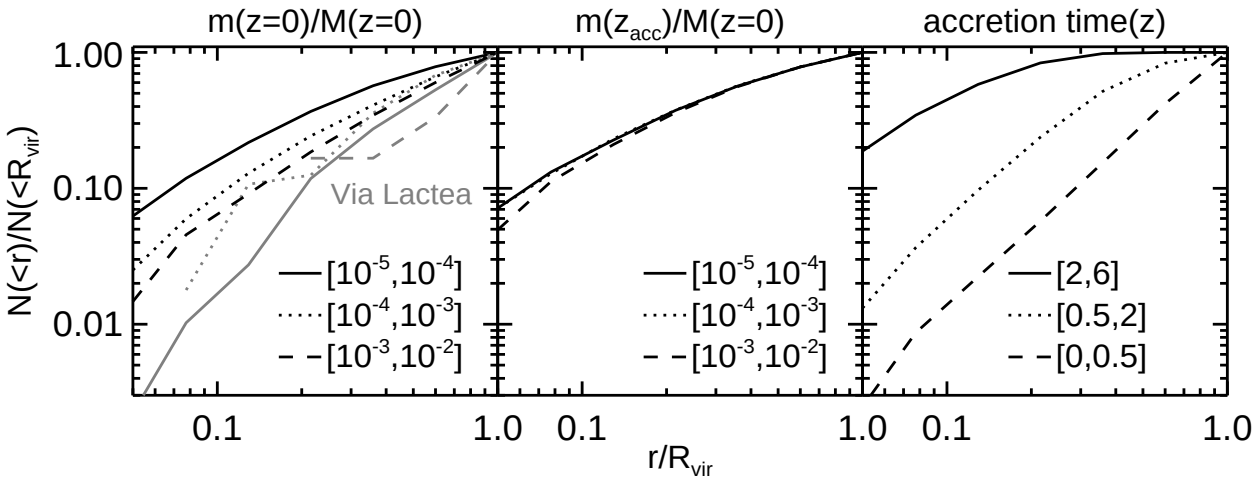

Figure 9. The dependence of subhalo radial distribution on subhalo properties. The left, middle and right panels show the dependence on the present-day mass, mass at accretion of subhaloes (both in unit of present host halo mass, as indicated in each panel) and their accretion redshift. In left panel, it also shows the distribution from the data of "Via Lactea" simulation as in grey lines.

present-day mass (left panel), mass at accretion (middle panel) and accretion redshift (right panel). The subhaloes mass are in unit of host halo mass at $z = 0$, and are indicated in each panel. In the left panel, the grey lines are the results obtained from the public data of "Via Lactea" simulation[6], where only the dependence on subhalo present-day mass can be derived.

The left panel shows that the radial distribution has a weak dependence on the present-day mass of subhalo. This is consistent with the results of De Lucia et al. (2004). Interestingly, the "Via Lactea" simulation show an opposite trend that higher-mass subhaloes have a more concentrated distribution within $r < 0.2R_{vir}$. As "Via Lactea" simulated only one host halo, there is significant scatter on the radial distribution of subhaloes due to the limited number in given mass bins. When split by their initial mass (i.e., mass at accretion), the subhaloes have almost the same radial distribution, as shown in the middle panel. This result also demonstrates that why the ridial distribution of suhaloes is independent of the dynamical processes (panel e and f of Fig. 8), as the subhaloes catalogue is dominated by the less massive suhaloes. The right panel shows that there is a significant dependence on the age of subhaloes that the old population has a more concentrated distribution at small radius. This age-dependence was also found by Taylor & Babul (2005b), and they pointed out that this is because old subhaloes are accreted at lower distances when the host halo was smaller at high redshift.

4 HALO OCCUPATION DISTRIBUTION OF SUBHALOES

In order to further examine the validity of our model, we investigate the halo occupation distribution (HOD) of subhaloes. For this purpose, we produce subhalo population in a set of host haloes with mass $M(z = 0) = 10^{11}, 10^{12}, 10^{13}, 10^{14}, 10^{15} h^{-1} M_{\odot}$. For each host halo, we produce 100 realizations of the merger trees, with a resolution of $10^7, 10^8, 10^9, 10^{10}, 10^{11} M_{\odot}$, respectively. The fiducial model M2 is used to model the evolution of each subhalo. We count the surviving subhaloes (N) in each realization and compute the quantity

$$\alpha \equiv \frac{\langle N(N-1)\rangle^{1/2}}{\langle N\rangle} \tag{16}$$

for each host halo. The quantity α is the normalized second moment of subhalo's HOD (e.g., Kravtsov et al. 2004a; van den Bosch et al. 2005). For a Poissonian distribution, α should be unity, while distributions that are narrower (sub-Poissonian) or broader (super-Poissonian) have $\alpha < 1$ and $\alpha > 1$, respectively. In the case of $\alpha \approx 1$ (i.e., small deviation of α from unity), one should keep in mind that it does not necessarily indicate a Poissonian statistics (e.g., Boylan-Kolchin et al. 2010) and it needs further examination on the subhalo's HOD. Here we use the quantity α only for a consis-

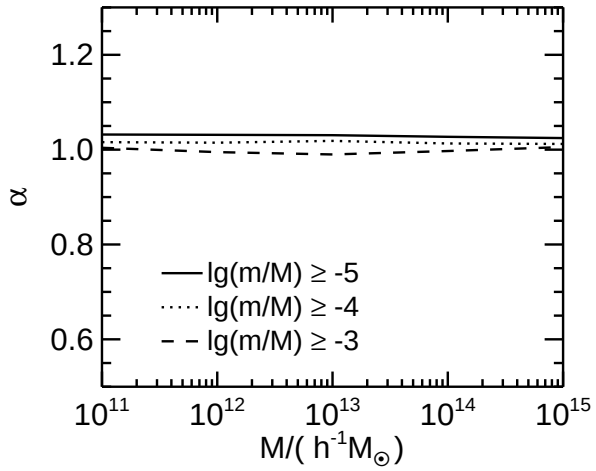

Figure 10. The normalized second moment of the HODs of subhaloes as a function of the host halo mass for three mass thresholds: $\lg m/M \geq -5, -4, -3$.

[6] http://www.ucolick.org/∼diemand/vl

tent comparison with the previous results (e.g., Z05; Zheng et al. 2005).

In Fig. 10 we plot α as function of the mass of the host halo. We select subhaloes with different mass bins of $\lg m/M \geq -5, -4, -3$. Fig. 10 shows that α is close to unity independent of the mass threshold and the host halo mass. This result is inconsistent with the semi-analytical result of van den Bosch et al. (2005) and Z05, who found that the distributions of massive subhaloes in low-mass host haloes are significantly broader than Poissonian distribution. They pointed out that the discrepancy may be from the generic problem of conventional EPS formalism. However, our model predictions agree with the numerical results of Kravtsov et al. (2004a) and Zheng et al. (2005). We argue that this is due to the improvement of our model in two folds. Firstly, we employ a modified EPS formalism by Parkinson et al. (2008) which is shown to produce a well math to the merger history of haloes found from N-body simulations. Secondly, we assume that subhaloes never get disrupted but are cannibalized with a time scale $T_{\rm df}$ (Fig. 6). It gives a better match to the observed distribution of satellite galaxies.

5 DISCUSSION

We have shown in Section 3.2 that the model predicts a more concentrated distribution of subhaloes than that seen from N-body simulations. This prediction is insensitive to the model assumptions for tidal stripping and dynamical parameters. The same discrepancy was also obtained by Taylor & Babul (2005), and they ascribed it to the numerical effects of simulations. The recent high-resolution N-body simulations (e.g., Springel et al. 2008) have shown that resolution is not the scapegoat for the low number density of subhaloes in the inner host halo. As pointed by Z05 that it is not the resolution but the model assumption that gives to the over-prediction. Z05 obtained a good match to the simulation result by implementing disruption of subhalo. Wetzel & White (2010) also have shown that decreasing the threshold of tidal disruption produces more subhaloes in the inner host halo.

We believe that the good agreement between our model prediction and the observed distribution of the MW satellites is a coincidence. To get a better match to the distribution of subhaloes from N-body simulations, we should firstly understand the importance of subhalo-subhalo interaction and subhalo-host interaction for the disruption of subhaloes, and more studies are needed to classify their contribution to this discrepancy. If these interactions are not enough to dissolve subhaloes in the inner host halo, a more realistic model for subhalo disruption should be included in the model. Currently, this is difficult to implement it. In one aspect, we need a more realistic and physical model for subhalo disruption, unlike those models to define disruption when the distance of subhalo to host center is less than some given radius because it is arbitrary and dependent on the resolution of simulations. On the other hand, subhalo disruption is easily to be confused with subhalo merging with central halo, which is often true for low-resolution simulations. For our experiment in this paper, we have to neglect the disruption and define subhalo merger using its angular momentum. This is adopted for making a fair comparison with the simulations of BK08.

Though we have neglected subhalo disruption in our model, the result indicates that disruption is not important for real galaxies. This is seen from panel d of Fig.8. Indeed, Hydrodynamical simulations with baryon included have confirmed that subhalo can survive the strong tidal disruption (e.g., Gnedin et al. 2004; Nagai & Kravtsov 2005; Weinberg et al. 2008; Dolag et al. 2009), and the predicted spatial distribution of satellite galaxies is similar to that observed in galaxy clusters (e.g., Gao et al. 2004a). Actually this is not the only solution to this problem. Some have argued that observed satellites in the MW are biased tracers of subhaloes (e.g., Kravtsov et al. 2004b; Madau et al. 2008). The readers are referred to the review paper by Kravtsov (2010) for more discussions.

6 CONCLUSION

In this paper, we study the evolution of dark matter subhalo using an analytical model including simple descriptions for a few important processes, such as tidal stripping, dynamical friction, tidal heating. We tune the model parameters to fit the dynamical evolution of subhalo predicted by controlled N-body simulation. Then we combine these descriptions with merger trees from the EPS-based Monte-Carlo merger trees and study the subhalo population in a Milky-Way type halo, including the subhalo mass function and the radial distribution of subhaloes.

Following Boylan-Kolchin et al. (2008), we define subhalo to be merged with central halo when its angular momentum reaches zero. We compare the predicted angular momentum evolution to the simulation results of BK08. We find that the mass loss of subhalo due to tidal stripping has great impact on its angular momentum evolution. A high tidal stripping efficiency, A, produces a fast decrease of subhalo mass and a longer merger time scales. We further find that the mass of subhalo should not decrease continuously by tidal stripping, and better agreement with simulation can be obtained if the mass of subhalo keep fixed after two passage of pericenter. We give a modified Coulomb logarithm using the fitting formula of BK08 to gain a well match to the subhalo merger time-scales.

We compare the subhalo mass function to that from N-body simulations, and it is found that SHMF is mainly determined by the tidal stripping efficiency A, but dependent weakly on the Coulomb logarithm parameters. It is also insensitive to subhalo mass loss at its late stage of evolution, as the SHMF is dominated by recently accreted subhaloes. This is in good agreement with the results of van den Bosch et al. (2005) and Yang et al. (2009).

The radial distribution of subhaloes is found to be more central concentrated than that from N-body simulations. This is a common prediction from analytical models if subhalo disruption is not important (Taylor & Babul 2005b; Z05; Wetzel & White 2010). N-body simulations (e.g., Gao et al. 2004b; Springel et al. 2008) seems to indicate that resolution is not the scapegoat for the under-prediction of subhaloes at small radii. The interaction between subhalo and host halo is efficient to eject small subhaloes into the outer region of host halo (Ludlow et al. 2009) which can

partly resolves this discrepancy. To fully solve this problem, we need a more physical model for subhalo disruption and distinguish between disruption and merger, which are not feasible at the moment.

We conclude that the better agreement between predicted spatial distribution of subhaloes and observed satellites in the Milky-Way is a coincidence. But it also implies that real galaxy may not be tidally disrupted, as found from hydrodynamical simulations (e.g., Dolag et al. 2009) that condensation of baryon mass inside subhalo will increase the central density of subhalo, making it more resistant to tidal disruption. Another argument for the concentrated distribution of satellite galaxies is that they are biased population of subhaloes found from simulations (e.g., Madau et al. 2008). A final solution to this issue should turn to the hydrodynamical simulation with high enough resolution and more realistic models for gas cooling and star formation in subhaloes.

Finally, we investigate the halo occupation distribution (HOD) of subhaloes with our improved model. The second moment of the HODs is close to unity, which disagrees with the results from semi-analytical model of van den Bosch et al. (2005) and Z05 but agrees with the HOD derived from numerical simulation by Kravtsov et al. (2004a) and Zheng et al. (2005).

ACKNOWLEDGEMENTS

JLG acknowledges the financial supports from Chinese Academy of Sciences and Max-Planck-Institute for Astronomy. We thanks Stelios Kazantzidis, Liang Gao and Guoliang Li for helpful discussions. We also thanks the referee for useful comments. XK is supported by the *One Hundred Talents* project of the Chinese Academy of Sciences and by the foundation for the author of CAS excellent doctoral dissertation. JLH is supported by the National Science Foundation of China under grant No. 10573028, the Key Project No. 10833005, the Group Innovation Project No. 10821302, and by 973 program No. 2007CB815402.

REFERENCES

Angulo, R. E., Lacey, C. G., Baugh, C. M., & Frenk, C. S. 2009, MNRAS, 399, 983
Benson, A. J., Lacey, C. G., Baugh, C. M., Cole, S., & Frenk, C. S. 2002, MNRAS, 333, 156
Benson, A. J. 2005, MNRAS, 358, 551
Binney, J., & Tremaine, S. 1987, Princeton, NJ, Princeton University Press, 1987, 747 p. (BT87)
Bond, J. R., Cole, S., Efstathiou, G., & Kaiser, N. 1991, ApJ, 379, 440
Boylan-Kolchin, M., Ma, C.-P., & Quataert, E. 2008, MNRAS, 383, 93 (BK08)
Boylan-Kolchin, M., Springel, V., White, S. D. M., & Jenkins, A. 2010, MNRAS, 827
Bryan, G. L., & Norman, M. L. 1998, ApJ, 495, 80
Bullock, J. S., Kolatt, T. S., Sigad, Y., Somerville, R. S., Kravtsov, A. V., Klypin, A. A., Primack, J. R., & Dekel, A. 2001, MNRAS, 321, 559
Bullock, J. S., & Johnston, K. V. 2005, ApJ, 635, 931
Chandrasekhar, S. 1943, ApJ, 97, 255
Cole, S., & Lacey, C. 1996, MNRAS, 281, 716
Colpi, M., Mayer, L., & Governato, F. 1999, ApJ, 525, 720
De Lucia, G., Kauffmann, G., Springel, V., White, S. D. M., Lanzoni, B., Stoehr, F., Tormen, G., & Yoshida, N. 2004, MNRAS, 348, 333
Diemand, J., Moore, B., & Stadel, J. 2004, MNRAS, 352, 535
Diemand, J., Kuhlen, M., & Madau, P. 2007a, ApJ, 657, 262
Diemand, J., Kuhlen, M., & Madau, P. 2007b, ApJ, 667, 859
Dolag, K., Borgani, S., Murante, G., & Springel, V. 2009, MNRAS, 399, 497
Fellhauer, M., & Lin, D. N. C. 2007, MNRAS, 375, 604
Gao, L., De Lucia, G., White, S. D. M., & Jenkins, A. 2004a, MNRAS, 352, L1
Gao, L., White, S. D. M., Jenkins, A., Stoehr, F., & Springel, V. 2004b, MNRAS, 355, 819
Giocoli, C., Tormen, G., & van den Bosch, F. C. 2008, MNRAS, 386, 2135
Giocoli, C., Tormen, G., Sheth, R. K., & van den Bosch, F. C. 2010, MNRAS, 342
Gnedin, O. Y., Kravtsov, A. V., Klypin, A. A., & Nagai, D. 2004, ApJ, 616, 16
Hashimoto, Y., Funato, Y., & Makino, J. 2003, ApJ, 582, 196
Hayashi, E., Navarro, J. F., Taylor, J. E., Stadel, J., & Quinn, T. 2003, ApJ, 584, 541
Jardel, J. R., & Sellwood, J. A. 2009, ApJ, 691, 1300
Jiang, C. Y., Jing, Y. P., Faltenbacher, A., Lin, W. P., & Li, C. 2008, ApJ, 675, 1095
Kang, X., Jing, Y. P., Mo, H. J., Börner, G. 2005, ApJ, 631, 21
Kang, X., 2008, arXiv: 0806.3279
Katz, N., & White, S. D. M. 1993, ApJ, 412, 455
Kazantzidis, S., Magorrian, J., & Moore, B. 2004a, ApJ, 601, 37
Kazantzidis, S., Mayer, L., Mastropietro, C., Diemand, J., Stadel, J., & Moore, B. 2004b, ApJ, 608, 663
Khochfar, S., & Burkert, A. 2006, A&A, 445, 403
Kim, H.-S., Baugh, C. M., Cole, S., Frenk, C. S., & Benson, A. J. 2009, MNRAS, 400, 1527
King, I. 1962, AJ, 67, 471
Klypin, A., Gottlöber, S., Kravtsov, A. V., & Khokhlov, A. M. 1999, ApJ, 516, 530
Kravtsov, A. V., Berlind, A. A., Wechsler, R. H., Klypin, A. A., Gottlöber, S., Allgood, B., & Primack, J. R. 2004a, ApJ, 609, 35
Kravtsov, A. V., Gnedin, O. Y., & Klypin, A. A. 2004b, ApJ, 609, 482
Kravtsov, A. 2010, Advances in Astronomy, 2010,
Kroupa, P., Theis, C., & Boily, C. M. 2005, A&A, 431, 517
Lacey, C., & Cole, S. 1993, MNRAS, 262, 627
Ludlow, A. D., Navarro, J. F., Springel, V., Jenkins, A., Frenk, C. S., & Helmi, A. 2009, ApJ, 692, 931
Macciò, A. V., Moore, B., Stadel, J., & Diemand, J. 2006, MNRAS, 366, 1529
Macciò, A. V., Kang, X., Fontanot, F., Somerville, R. S., Koposov, S. E., & Monaco, P. 2009, arXiv:0903.4681
Madau, P., Diemand, J., & Kuhlen, M. 2008, ApJ, 679, 1260
Martin, N. F., de Jong, J. T. A., & Rix, H.-W. 2008, ApJ, 684, 1075
Mateo, M. L. 1998, ARA&A, 36, 435
Metz, M., Kroupa, P., & Jerjen, H. 2007, MNRAS, 374, 1125
Metz, M., Kroupa, P., & Jerjen, H. 2009, MNRAS, 394, 2223
Moore, B., Ghigna, S., Governato, F., Lake, G., Quinn, T., Stadel, J., & Tozzi, P. 1999, ApJL, 524, L19
Nagai, D., & Kravtsov, A. V. 2005, ApJ, 618, 557
Navarro, J. F., Frenk, C. S., & White, S. D. M. 1995, MNRAS, 275, 56
Navarro, J. F., Frenk, C. S., & White, S. D. M. 1997, ApJ, 490, 493
Neto, A. F., et al. 2007, MNRAS, 381, 1450
Parkinson, H., Cole, S., & Helly, J. 2008, MNRAS, 383, 557

Peñarrubia, J., Navarro, J. F., & McConnachie, A. W. 2008, ApJ, 673, 226
Somerville, R. S., & Kolatt, T. S. 1999, MNRAS, 305, 1
Springel, V., White, S. D. M., Tormen, G., & Kauffmann, G. 2001, MNRAS, 328, 726
Springel, V., et al. 2008, MNRAS, 391, 1685
Taffoni, G., Mayer, L., Colpi, M., & Governato, F. 2003, MNRAS, 341, 434
Taylor, J. E., & Babul, A. 2001, ApJ, 559, 716
Taylor, J. E., & Babul, A. 2004, MNRAS, 348, 811
Taylor, J. E., & Babul, A. 2005a, MNRAS, 364, 515
Taylor, J. E., & Babul, A. 2005b, MNRAS, 364, 535
Toomre, A., & Toomre, J. 1972, ApJ, 178, 623
Tormen, G. 1997, MNRAS, 290, 411
Tormen, G., Diaferio, A., & Syer, D. 1998, MNRAS, 299, 728
van den Bosch, F. C., Tormen, G., & Giocoli, C. 2005, MNRAS, 359, 1029
Velazquez, H., & White, S. D. M. 1999, MNRAS, 304, 254
von Hoerner, S. 1957, ApJ, 125, 451
Weinberg, D. H., Colombi, S., Davé, R., & Katz, N. 2008, ApJ, 678, 6
Wetzel, A. R., & White, M. 2010, MNRAS, 403, 1072
White, S. D. M. 1976, MNRAS, 174, 467
Willman, B., Governato, F., Dalcanton, J. J., Reed, D., & Quinn, T. 2004, MNRAS, 353, 639
Yang, X., Mo, H. J., & van den Bosch, F. C. 2009, ApJ, 693, 830
Zentner, A. R., & Bullock, J. S. 2003, ApJ, 598, 49
Zentner, A. R., Berlind, A. A., Bullock, J. S., Kravtsov, A. V., & Wechsler, R. H. 2005, ApJ, 624, 505 (Z05)
Zheng, Z., et al. 2005, ApJ, 633, 791